Earthq Eng & Eng Vib (2019) 18: 433-446 **DOI**: https://doi.org/10.1007/s11803-019-0486-9

Seismic performance evaluation of typical dampers designed by Chinese building code

Guo Wei[1, 2†], Wu Jun[3‡], Hu Yao[1, 2‡], Li Yunsong[3] , Yang T.Y.[4†]

1. *School of Civil Engineering, Central South University, Changsha 410075, China*

2. *National Engineering Laboratory for High Speed Railway Construction, Changsha 410075, China*

3. *Department of Structural Engineering, Tongji University, Shanghai 200092, China*

4. *Department of Civil Engineering, University of British Columbia, Vancouver, Canada*

Abstract: Adding dampers is a commonly adopted seismic risk mitigation strategy for modern buildings, and the corresponding design procedure of dampers has been well established by the Chinese Building Code. Even though all types of dampers are designed by the same procedure, actual seismic performance of the building may differ from one to the others. In this study, a nine-story benchmark steel building is established, and three different and typical types of dampers are designed according to the Chinese Building Code to realize structural vibration control under strong earthquake excitation. The seismic response of the prototype building equipped with a viscoelastic damper, viscous damper and buckling-restrained brace (BRB) subjected to 10 earthquake records are calculated, and Incremental Dynamic Analysis (IDA) is performed to describe progressive damage of the structure under increasing earthquake intensity. In the perspective of fragility, it shows that the viscoelastic damper has the highest collapse margin ratio (CMR), and the viscous damper provides the best drift control. Both the BRB and viscoelastic dampers can effectively reduce the floor acceleration responses in the mid-rise building.

Keywords: Chinese building design code; viscoelastic damper; viscous damper; buckling-restrained brace; seismic response; fragility analysis

1 Introduction

Recent huge earthquakes worldwide have caused significant structural collapse and nonstructural damage, and generally large financial losses follow. For example, the 2008 Wenchuan earthquake (Zhao *et al.*, 2009) led to nearly 100,000 fatalities and $130 billion USD financial losses. The 2011 Tohoku Japan earthquake (Zhou *et al.*, 2012) destroyed a significant portion of Eastern Japan and caused $200 billion USD in financial losses. Since the concept of structural control was proposed in the 1970s (Kelly *et al.*, 1972), rapid development began in China. A variety of energy dissipation systems have been studied systematically, such as metallic dampers (Li and Li, 2004, Li and Li, 2007), lead viscoelastic dampers (Zhou *et al.*, 2001), pall-typed frictional dampers (Wu *et al.*, 2005) and a new typed of BRB (Sun *et al.*, 2011, Zhao *et al.*, 2011). And tuned mass damper (Guo *et al.*, 2012) is also considered to be a special damper.

These typical types of dampers have been implemented in buildings and bridges to prevent the earthquake-induced pounding (Yu *et al.*, 2017) and damage, and much more innovative dampers are still being developed. As dampers usually provide additional damping to structure to absorb energy, which possess non-proportional damping characteristic, special calculation methods (Guo *et al.*, 2010, Guo *et al.*, 2011, Guo *et al.*, 2013, Guo *et al.*, 2013, Liu *et al.*, 2010) have been proposed. Also, several theoretical and experimental research studies have been conducted to investigate the influence of different dampers on the system response behavior. Kasai *et al.* (2009) evaluated the seismic performance of a five-story building with several types of commercially available dampers through full-scale shaking table tests. The dampers include viscous, oil, viscoelastic and steel dampers. The tests give the hysteresis curves of these four dampers by which a numerical analysis is performed. In the tests, the practical performance of a mid-rise steel building is confirmed by inputting minor, major

Correspondence to: Guo Wei, School of Civil Engineering, Central South University, Changsha 410075, China
Tel: +86-731-82655366
E-mail: wei.guo.86@foxmail.com
†Associate Professor; ‡Master student

Supported by: National Natural Science Foundation of China under Grant No. 51108466, Development Program for Changjiang scholars and innovative team under Grant No. IRT1296 and the Project of Innovation-Driven Plan in Central South University

Received May 7, 2017; **Accepted** September 27, 2018

and catastrophic (Kobe) ground motions, and it can be seen that most of the frame members remain elastic, which benefits the numerical modeling by relative simple and clear mathematical equations. Chang *et al.* (2008) studied a seismic retrofit method of existing buildings using nonlinear viscous dampers, in which a shaking table test was conducted for verification. Fu and Kasai (1998) studied the performance change of frames using viscoelastic and viscous dampers through deterministic methods, by which it can be concluded that the viscoelastic damper is better in controlling of peak displacement response.

As of today, several Chinese Building Design Codes, such as the Code for Seismic Design of Buildings (GB50010-2010) (CSDB) and Technical Specification for Seismic Energy Dissipation of Buildings (JGJ297-2013) (TSSE), have been well established to provide guidance for damper design in China. The American building code guidelines (ASCE-7-10), FEMA-P695 (2009) and SEAOC (1995) have also described the design methods of dampers adopted in United States, and ASCE 41 (ASCE, 2013) provides the seismic evaluation method of existing buildings which can be used for performance analysis of dampers. It can be considered that damper technology has relatively matured and has been well applied in seismic response control of buildings. However, it is also apparent that even though the different types of dampers are designed based on the same code and objectives, there may be distinct differences in effectiveness of structural response under the same earthquake time history excitation because of the variation of the damping mechanism. Further research is still required to quantify the validity of seismic response control of typical types of dampers designed by the same codes and the ability to mitigate the probability of structural collapse or device damage. As the earthquake occurs randomly, it is also essential to statistically study the performance of dampers to realize a fragility analysis.

In this study, the Chinese Building Design Code is used to design three different types of dampers installed in a nine-story steel benchmark building (Ohtori *et al.*, 2004), and the three types of dampers adopt the same design performance objective. Both the Chinese code and (ASCE-7-10) are introduced to evaluate and select 10 earthquake records from the PEER Center. The seismic response of the prototype building equipped with a viscoelastic damper, viscous damper and buckling-restrained brace (BRB) subjected to 10 earthquake records are studied systematically using the software Opensees, which is very powerful to fine simulate the seismic response of building, bridge, and moving train on bridge (Gu *et al.*, 2018; Hou *et al.*, 2018). Then, by Incremental Dynamic Analysis (IDA) and seismic fragility analysis, the corresponding damage states under multiple earthquake magnitudes are described statistically. The results can provide a guide for designers to select the appropriate type of damper when all dampers well designed by codes seem to present nearly the same performance of response control.

2 Damper designed by Chinese code

2.1 Effective damping ratio

TSSE (JGJ297-2013) explicitly outlines the damper design procedure currently used in practice in China. The procedure follows the concept that the additional stiffness and damping damper are equivalent to the effective structural stiffness and effective damping ratio under a frequent earthquake. According to the TSSE, the effective stiffness can be calculated using the secant stiffness corresponding to the maximum displacement of a given dampers hysteresis curve. The effective damping ratio can be identified by Eq. (1) as follows:

$$\xi_{\mathrm{d}} = \sum_{j=1}^{n} W_{\mathrm{c}j} / 4\pi W_{\mathrm{s}} \tag{1}$$

where

$W_{\mathrm{s}} = \sum F_i u_i / 2$; $W_{\mathrm{c}j1} = \left(2\pi^2 / T_1\right) \sum C_j \cos^2\theta_j \Delta u_j^2$;
$W_{\mathrm{c}j2} = \sum A_j$

in which F_i is the horizontal shear force at the ith floor; u_i is the horizontal displacement at the ith floor; T_1 is the natural period of structure; Δu_j is the inter-story displacement at the jth floor; W_{s} is the total strain energy under the horizontal earthquake excitation; $W_{\mathrm{c}j1}$ is the energy consumed by the jth linear viscous or viscoelastic damper of the structure in a full cycle with the target inter-story displacement, and $W_{\mathrm{c}j2}$ is the energy consumed by other types such as BRB. In the above equation, $W_{\mathrm{c}1j}$ corresponds to a viscous damper installed in the benchmark model to provide the effective damping ratio, and $W_{\mathrm{c}2j}$ corresponds to viscoelastic dampers and $W_{\mathrm{c}3j}$ is BRB. C_j is the damping coefficient of the jth dampers; θ is the angle between the motion direction of dampers and the horizontal direction, and A_j is the area of the hysteretic loop at the inter-story displacement of the jth damper. According to CSDB (GB50010-2010), it is apparent that the design method to calculate the effective stiffness and effective damping ratio is approximate and described in the linear formulation by adopting the first mode response. According to TSSE, the above equations are applicable to all dampers including nonlinear dampers. Furthermore, the dampers are not required to be placed at all levels, but do not make the stiffness distribution of the building very uneven. The stiffness from VE and BRB should be considered in the calculation.

2.2 Steel structure Benchmark model

The nine-story steel structure moment resisting frame developed by the SAC project is used as the

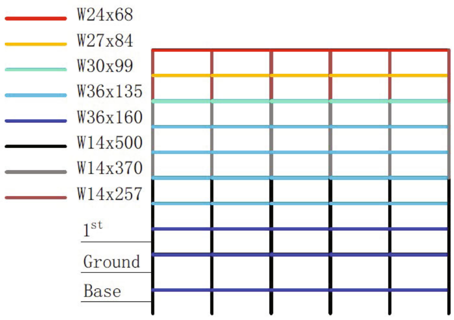

Mass (kg):	
Ground	9.65×10^5
1st	1.01×10^6
2nd-8th	9.89×10^5
9th	1.07×10^6
All	9.0×10^6
Height (m):	
Base	3.65
Ground	5.49
1st-8th	3.96
Bay widths (all) 9.15m	

Fig. 1 Nine-story steel structure *YZ* moment-resisting frame of the benchmark building (The first three periods of the model are: $T_1 = 2.28$ s, $T_2 = 0.828$ s, $T_3 = 0.4463$ s)

Benchmark building (Ohtori *et al.*, 2004) for this study. Suppose the building is located at an 8-degree seismic intensity zone. In the Chinese code CSDB (GB50010-2010), the seismic intensity (i.e. 10% probability of exceedance in 50 years) is used to describe the Seismic Ground Motion Parameter Zonation Map of China, from 6-degree to 9-degree. The site is supposed to be site-class II and the second group, in which the equivalent shear-wave velocity of 30 m soil (V_{S30}) is between 250m/s and 500 m/s and the distance from the epicenter is medium distance. Figure 1 shows the summary of information of the prototype benchmark building.

Figure 2(a), 2(b), and 2(c) show the 3D rendering, elevation and plan view of the prototype benchmark model. The dampers are assumed to be located at the central bay of the building at all floors. Since the numerical model is symmetrical, the torsion response of the building can be neglected, and only its unidirectional vibration (*X* direction) is analyzed. The dampers are set along the *X* direction.

2.3 Hysteretic model of buckling restrained brace

Before designing the typical dampers, a reasonable model should be described and calibrated by the experiments, and then the parameters of the designed dampers can be considered to be logical and implemented in practical engineering.

First the design procedure in this study is based on the buckling restrain brace, so the authors refer to a TJI-type BRB (Sun *et al.*, 2011), which was developed at Tongji University. The hysteresis curve of the tested specimen is shown in Fig. 3. After detailed calibration, the Bouc-Wen model is used to simulate the BRB damper, and the fitting curve is shown in Fig. 4.

Once the material and the technics of the BRB are determined, the main design factor is the cross section; in other words, the initial elastic stiffness in the Bouc-Wen model should be designed. It is easy for designers to determine the physical parameters of the BRB by adjusting the initial elastic stiffness k_0 linearly. Then the designed dampers can be used to reduce the response to meet structural seismic demands.

2.4 Damper parameter design

In the process of designing three typical dampers, the top floor's displacement of the structure is chosen as the design control index, and the design target for all dampers is to reduce the top floor's displacement to 70% of the original values under the same seismic earthquake excitation. Figure 5 shows the flowchart of BRB damper's parameter design. In the process shown in Fig. 5, the effective stiffness K_d and effective damping ratio ξ_d provided by the dampers are calculated by iteration, through which continuously adjusting the BRB damper represented by the Bouc-Wen model can realize the design target of reducing the top displacement of the building to 70% of the original. Once the parameters K_d and ξ_d are obtained, they can be used to calculate the corresponding BRB's Bouc-Wen model, and furthermore can be referenced to determine the physical parameters

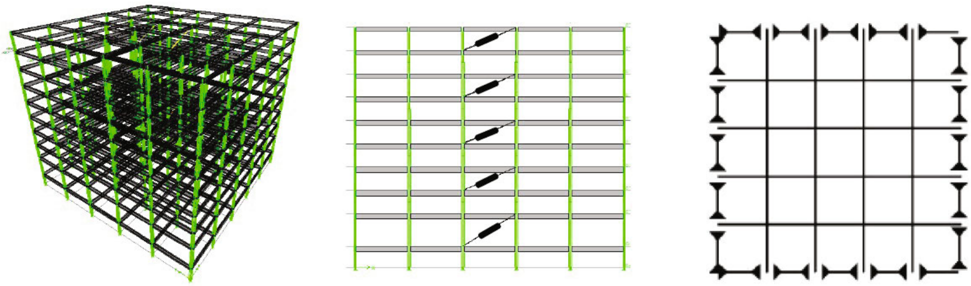

(a) 3D diagram (b) *XZ* elevation (c) *XY* plan view

Fig. 2 Nine-story steel structure benchmark model and dampers setting

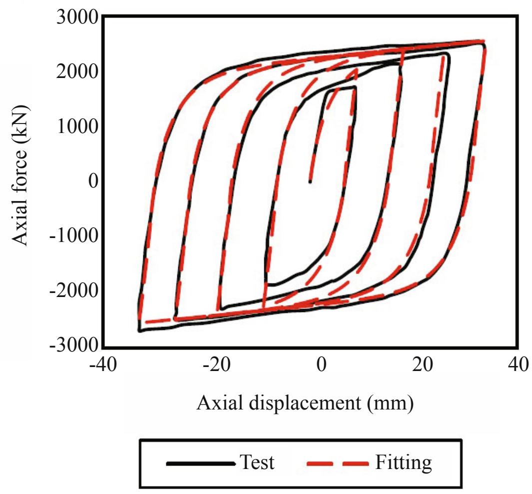

Fig. 3 Hysteresis curves of tested BRB

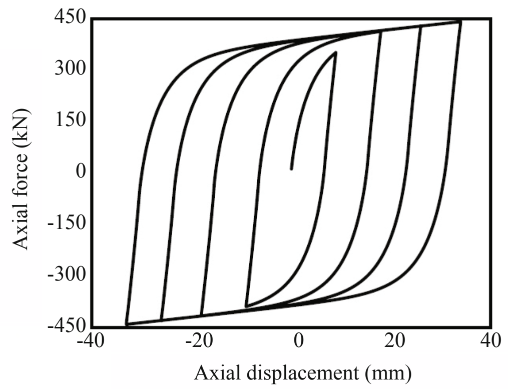

Fig. 4 Fitting curve of Bouc-Wen model

of the viscoelastic and viscous dampers.

In the design process, it is always assumed that all dampers are working under the first mode period, as the response behavior of the structure are primarily dominated by the first mode (Chang *et al.*, 2008), and the mass participation factor of the first mode of the benchmark model reaches over 80%. Based on this assumption, the sine-displacement excitation corresponding to the first period T_1 is given to calculate the dissipated energy W_{cj1}. However, there are slight differences between the structure with viscoelastic dampers and viscous dampers as viscous dampers actually present no stiffness. For viscoelastic dampers, the target is to obtain the stiffness K_{d} and the damping coefficient C_{d}. In order to simplify the calculation, the K_{d} and ξ_{d} is assumed to be equal to the BRB's effective parameters. Then, the linear damping coefficient C_{d} is calculated by the Eq. (1) with W_{cj1}. For viscous dampers, the parameter is C_{d} or ξ_{d}, therefore ξ_{d} is adjusted until the top displacement reduces to 70%. Table 1 shows the designed parameters of the viscoelastic damper, viscous damper and BRB damper. In the first column of the table, three hysteresis curves and corresponding equations are given. According to the TSSE (JGJ297-2013) and Fig. 5, the contribution of dampers to the structure can be divided into K_{d} and ξ_{d}, which is given in the second column. Once these two parameters are determined, the performance of the dampers can be calculated. The third column gives the specific values of each parameter in the equation. The parameters in Table 1 include the Bouc-Wen model's values used in Opensees to simulate physical dampers and the design effective stiffness and damping ratio, which is given by Chinese codes as shown in Fig. 5.

Furthermore, in order to verify the validity of the natural frequency of the structure model in the design, the static displacement numerical test is performed to calculate the approximate natural frequency T_1 of the structure with added BRBs or V-E dampers. The method is to apply the horizontal loads $\boldsymbol{P}$ proportional to the mass of each floor. Then the displacement of each floor, which can be written as $\boldsymbol{u}$ is calculated. Hence, the estimated natural frequency can be calculated as follows. If the calculated natural frequency does not equal the value adopted in the design, it should be modified for the damper design. However, in the design of the benchmark model in this study, the result is very close to the fundamental period of 2.12 seconds and the numerical model is reasonable.

$$\omega^2 = \frac{\boldsymbol{u}^T \boldsymbol{K}\boldsymbol{u}}{\boldsymbol{u}^T \boldsymbol{M}\boldsymbol{u}} = \frac{\boldsymbol{u}^T \boldsymbol{P}}{\boldsymbol{u}^T \boldsymbol{M}\boldsymbol{u}} = 8.458,\ T_1 = \frac{2\pi}{\omega} \approx 2.16\ \mathrm{s}. \tag{2}$$

3 Damper performance assessment

3.1 Select earthquake records

Ten earthquake ground motion records (GR) are selected from the Pacific Earthquake Engineering Research (PEER) NGA database (Chiou *et al.*, 2008). Table 2 shows the summary of the ground records used in the incremental dynamic analysis (IDA).

The ground motions are scaled according to the procedure similarly outlined in both frequency methods (Zhao, 2015) and ASCE-7-10. Three period ranges were considered. The first range is $\left[T_1 - \Delta T_1, T_1 + \Delta T_2\right]$, the second range is $\left[T_2 - \Delta T_1, T_2 + \Delta T_2\right]$, and the third range is $\left[0.2T_1, 1.5T_1\right]$, as shown in Table 3.

Figure 6 shows the scaled response spectra and design spectrum. The result shows that in the first frequency range, the scaled response spectrum is less than the design spectra with the 20% maximum deviation, in the second frequency range, the scaled response spectrum is in the interval which can satisfy the design demand, and in the third frequency range which covers most of the first and second ranges, the scaled response spectra is in good agreement with design spectra, where the maximum deviation is less than 30%. The two methods all demonstrate the reliability of the selected earthquake

Table 1 Hysteretic models and parameters of dampers

<table>
<tr><th></th><th>Hysteretic model</th><th>Design parameters According to TSSE</th><th>Hysteretic curve's parameters Used in Opensees</th></tr>
<tr><td>(a)</td><td>
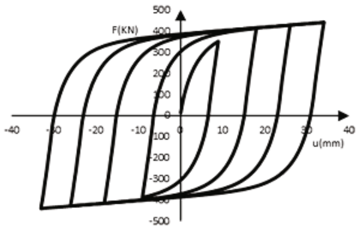

$$\Phi_{BW}(x,t) = \alpha kx(t) + (1-\alpha)Dkz(t)$$
$$\dot{z} = D^{-1}(A\dot{x} - \beta|\dot{x}||z|^{n-1}z - \gamma\dot{x}|z|^{n})$$
Bouc-wen model of BRB</td><td>$K_d = 5.2\times10^7$ N/m
$\xi_d = 0.0591$
$\xi_1 = 0.02$
$T_1 = 2.12$ s</td><td>$\alpha = 0.0085$
$k_0 = 1.9\times10^8$ N/m
$n = 0.4$
$\beta = 0.5,\ \gamma = 0.25$
$A_0 = 1$</td></tr>
<tr><td>(b)</td><td>
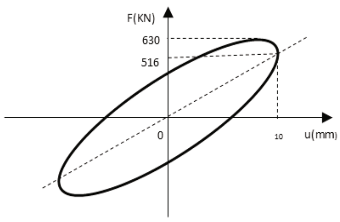

$$F = K_d u + C_d \dot{u}$$
Kelvin model of viscoelastic damper</td><td>$K_d = 5.2\times10^7$ N/m
$\xi_d = 0.0591$
$\xi_1 = 0.02$
$T_1 = 2.12$ s</td><td>$K_d = 5.2\times10^7$ N/m
$C_d = 3.7\times10^7$ N·s/m</td></tr>
<tr><td>(c)</td><td>
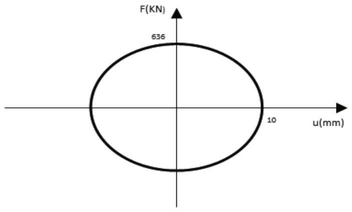

$$F = C_d \dot{u}^{\alpha}$$
Model of viscous damper</td><td>$\xi_d = 0.138$
$\xi_1 = 0.02$
$T_1 = 2.28$ s</td><td>$C_d = 3.7\times10^7$ N·s/m
$\alpha = 1$</td></tr>
</table>

Table 2 Earthquake ground motion records used for IDA

GR	Name	Year	Station	Magnitude
1	Imperial Valley-02	1940	EI Centro Array #9	6.95
2	San Fernando	1971	LA – Hollywood Stor FF	6.61
3	Imperial Valley-06	1979	EI Centro Array #13	6.53
4	Superstition Hills-02	1987	EI Centro Imp. Co. Cent	6.54
5	Loma Prieta	1989	Fremont – Mission San Jose	6.93
6	Landers	1992	Barstow	7.28
7	Kobe Japan	1995	Abeno	6.9
8	San Simeon CA	2003	San Luis Obispo	6.52
9	EI Mayor-Cucapah Mexico	2010	EI Centro – Meloland Geot. Array	7.2
10	Darfield New Zealand	2010	Canterbury Aero Club	7

Table 3 Frequency ranges used for selecting earthquake records

Damper	The 1st range	Accuracy	The 2nd range	Accuracy	The 3rd range	Accuracy
BRB	[1.92,2.62]	20%	[0.551,1.25]	20%	[0.424, 3.18]	30%
Viscoelastic	[1.92,2.62]	20%	[0.551,1.25]	20%	[0.424, 3.18]	30%
Viscous	[2.08,2.78]	20%	[0.628,1.33]	20%	[0.456, 3.42]	30%

Note: The periods of the building with BRB, viscoelastic and viscous dampers are, respectively, $T_1 = 2.12$ s, 2.12 s, 2.28 s; $T_2 = 0.751$ s, 0.751 s, 0.828 s; $T_3 = 0.412$ s, 0.412 s, 0.4463 s. $\Delta T_1 = 0.2$ s, $\Delta T_2 = 0.5$ s.

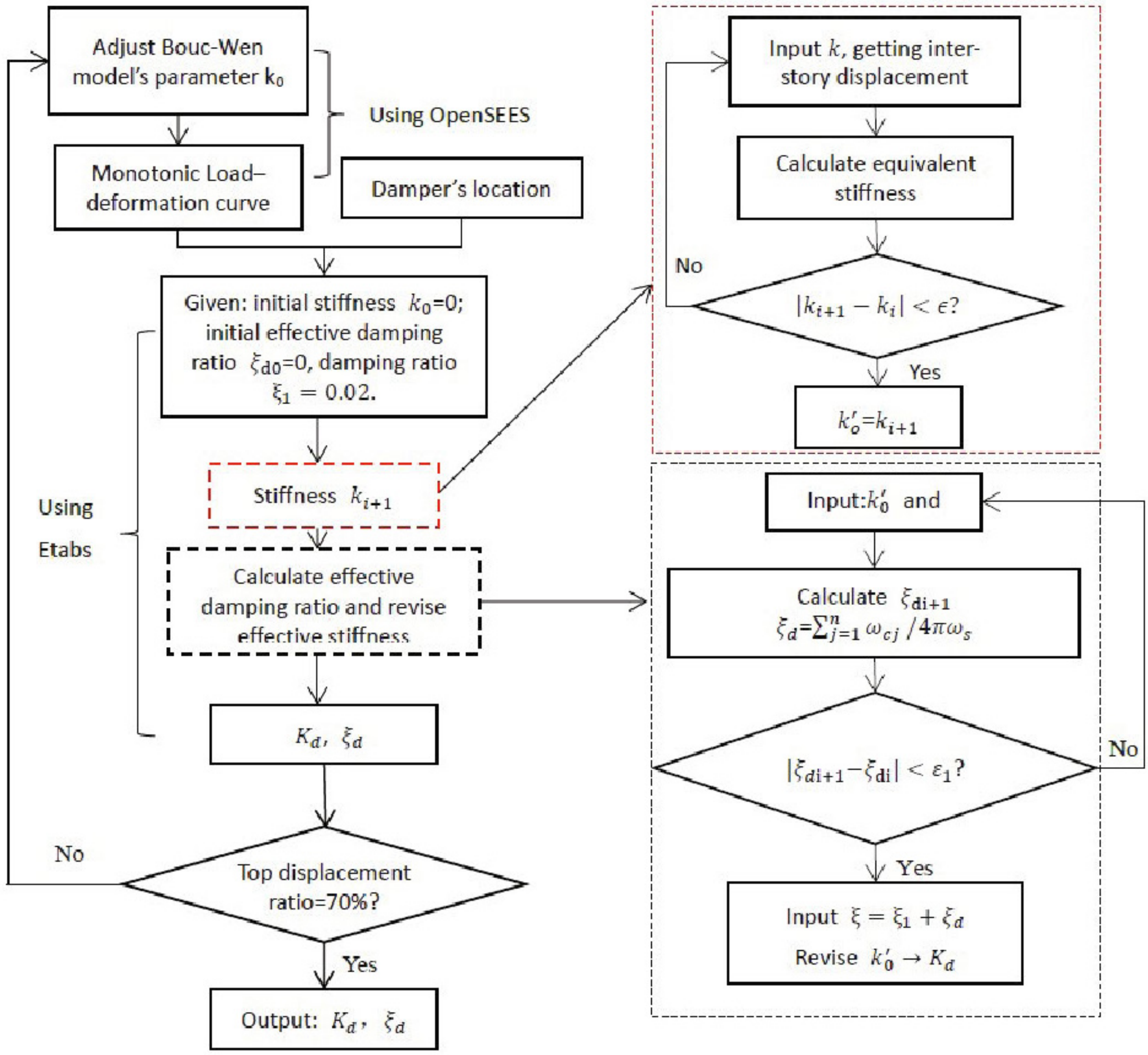

Fig. 5 Flowchart of BRB's parameter design

records.

The effective duration of selected earthquake records should also be checked. According to the Chinese code for the seismic design of buildings, the effective duration should be more than 5 to 10 times the natural period of the structure. Thus, herein, the selected earthquake records have a good reliability.

3.2 Performance assessment

3.2.1 Collapse assessment according to FEMA-P695 (2009)

Incremental Dynamic Analysis (IDA) (FEMA-P695, 2009) is adopted to calculate the seismic responses of the structure at different earthquake intensities. The values

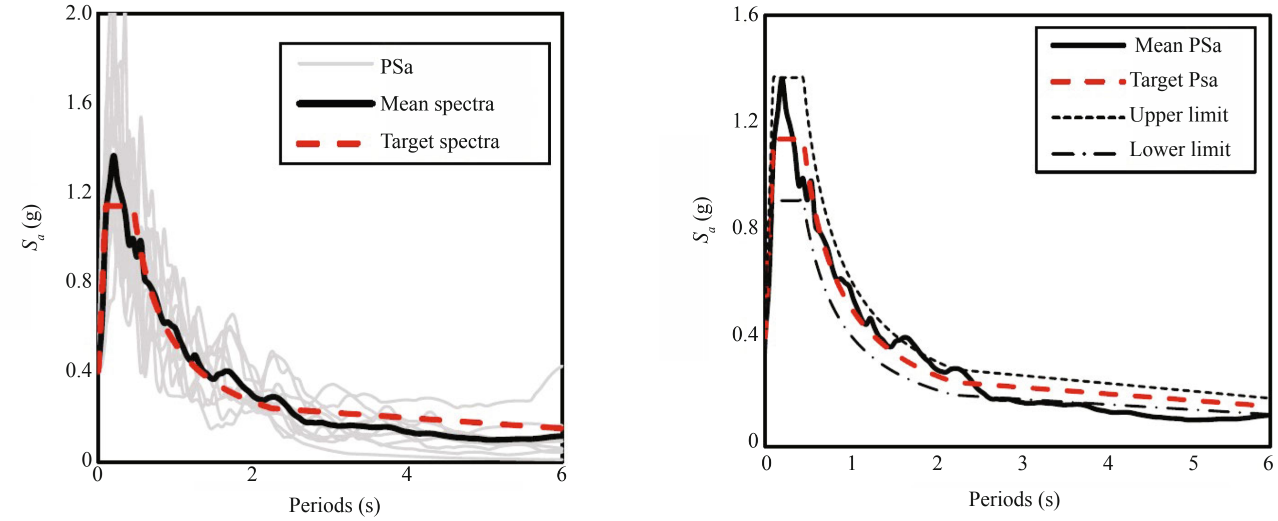

Fig. 6 (a) Ten GRs and the mean curve; (b) Mean and target spectra

Table 4 Drift limits related with performance in the CSDB

No damage	Slight damage	Moderate damage	Severe damage	Ultimate state
<$[\Delta u_e]$	<$2[\Delta u_e]$	<$4[\Delta u_e]$	<$[\Delta u_p]$	>$[\Delta u_p]$

Note: $\Delta u_e = 1/250$ is the upper limit of the elastic inter-story drift under frequent earthquake; $\Delta u_p = 1/50$ is the upper limit of the plastic inter-story drift under rare earthquake.

presented in Tables 5 and 6 are used to evaluate the structural damage situations by the performance limits. In addition, collapse of the structure is determined here when the IDA curve decreases to 20% of the initial slope.

Figures 7-9 give the IDA curves of the prototype building with supplemental BRB, viscoelastic and viscous dampers under 10 earthquake records. Figure 10 shows the IDA curves of the building without any dampers. Accordingly, the corresponding collapse fragility curves are presented in Fig. 11. In the fragility curves, the maximum spectral acceleration is about 1.0 g and the corresponding value of PGA is around 2.0 g-2.8 g because of the large natural period of the structure, which seems to be reasonable.

The result shows that when $S_a \leq 0.1$ g the structure has a very low probability of collapse, which is approximately <0.1%. However, when $S_a > 0.1$ g, the structure has a high probability of collapse for all three types of dampers, which is approximately near 100% of the collapse probability.

Table 5 Acceleration limits for several types of devices (Wang, 2005; Xiong, 2016)

Devices	Laboratory devices	Operation room devices	Voltage transformer
Limit acceleration (g)	0.15	0.5	0.79

Note: Voltage transformer's limit acceleration is derived by linear regression based on data of Wenchuan earthquake with damage probability of 50%

Table 6 Spectra acceleration S_a of structure with three types of dampers in different earthquake intensity

Structure-damper system (Liu *et al*., 2010)	Frequent earthquake ($\alpha_{max} = 0.16$ g)	Design earthquake ($\alpha_{max} = 0.45$ g)	Rare earthquake ($\alpha_{max} = 0.90$ g)
Structure-BRB	$S_a = 0.034$ g	$S_a = 0.096$ g	$S_a = 0.191$ g
Structure-viscoelastic damper	$S_a = 0.034$ g	$S_a = 0.096$ g	$S_a = 0.191$ g
Structure-viscous damper	$S_a = 0.029$ g	$S_a = 0.081$ g	$S_a = 0.162$ g

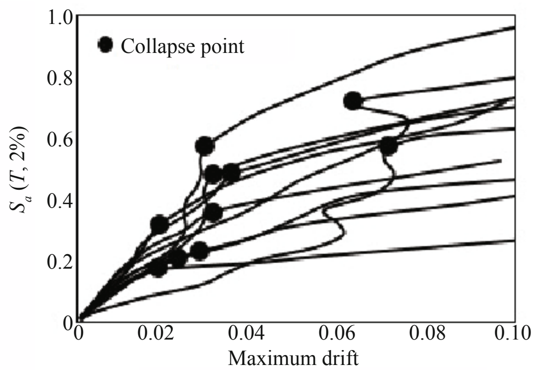

Fig. 7 IDA curves of structure with BRB dampers

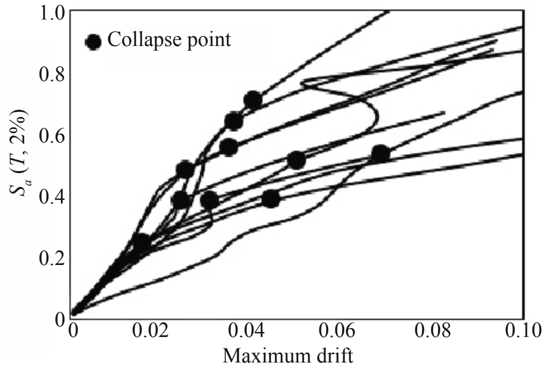

Fig. 8 IDA curves of structure with viscoelastic dampers

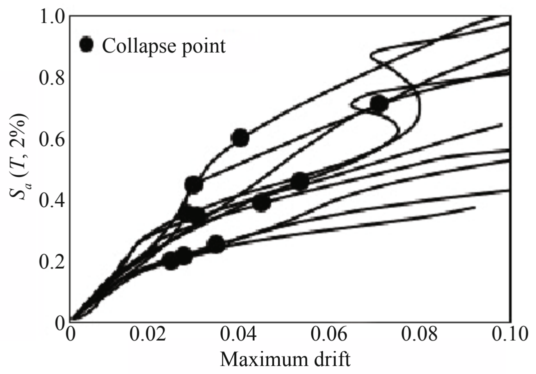

Fig. 9 IDA curves of structure with viscous dampers

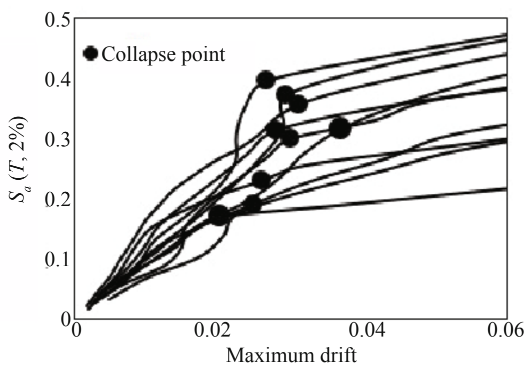

Fig. 10 IDAs of structure with no dampers

The collapse margin ratio (CMR) (FEMA-P695, 2009), which is defined as follows:

$$\mathrm{CMR} = \frac{\hat{S}_{\mathrm{CT}}}{S_{\mathrm{MT}}} \tag{3}$$

in which $\hat{S}_{\mathrm{CT}}$ is the median collapse intensity corresponds to a 50% probability of collapse; S_{MT} is the maximum considered earthquake (MCE) ground motion intensity of the specific seismic design category (SDC) and of the fundamental period (T) of the structure.

It can be easily calculated that S_{CT} of BRB, viscoelastic damper and viscous damper are 0.38 g, 0.47 g and 0.37 g, respectively, and S_{MT} of BRB, viscoelastic damper and viscous damper are 0.1913 g, 0.1913 g and 0.1621 g, respectively. The result shows that the CMR are 1.97, 2.46 and 2.28, for the BRB, viscoelastic and viscous damper installed structure, respectively. According to FEMA P695 (FEMA-451), the adjusted collapse margin ratio (ACMR) is calculated to estimate the anti-collapse performance. The ACMR of the system is calculated as follows:

$$\mathrm{ACMR} = \mathrm{CMR} \times \mathrm{SSF} \tag{4}$$

$$\mathrm{SSF} = \exp\left[\beta_1(T) \times \left(\bar{\varepsilon}_0 - \bar{\varepsilon}(T)\right)\right] \tag{5}$$

in which SSF is defined as the spectral shape factor;

$\beta_1(T) = 0.14 \times (\mu_T - 1)^{0.42} \le 0.317$;

$\bar{\varepsilon}(T) = 1.0$ for seismic design categories (SDC) B and C, 1.5 for SDC D, 1.2 for SDC E

$\bar{\varepsilon}(T) = 0.6 \times (1.5 - T), \bar{\varepsilon} = 0.6$ if $T \le 0.5$ and $\bar{\varepsilon} = 0.0$ if $T \ge 1.5$

The result shows the ACMR are 2.363, 2.950 and 2.734 of the BRB, viscoelastic and viscous dampers,

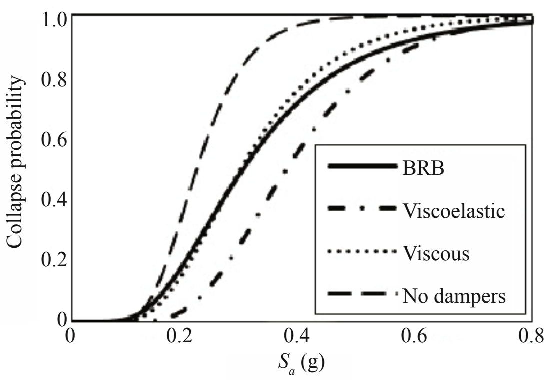

Fig. 11 Collapse fragility curves

respectively. It indicates that the viscoelastic damper has the best performance in collapse control of the structure.

3.2.2 Performance control according to CSDB

Table 4 and Table 5 show the displacement and acceleration target performance limits as defined in CSDB (GB50010-2010). These values are used to quantify the state of the structural performance.

Figures 12(a), 13(a) and 14(a) show the fragility curves of the building with the BRB, viscoelastic and viscous dampers, respectively. Similarly, Figs. 12(b), 13(b) and 14(b) show the probability of the damage states for the structure with the BRB, viscoelastic and viscous dampers, respectively.

From Figs. 12(b), 13(b) and 14(b), the performances of the structure with three types of dampers under three levels of earthquake intensities can be compared in detail, which is shown in Figs. 15-17. For convenience of discussion and explanation, the spectra acceleration S_a, of these dampers in frequent, design, and rare earthquake intensities are shown in Table 6.

In Table 6, α_{max} denotes the maximum acceleration value of the design response spectra according to the Code for Seismic Design of Buildings (GB50010-2010). The values of S_a of three structure-damper systems are calculated according to the design response spectra (GB50010-2010) with the parameters $\xi_d + \xi_1$ and T_1 shown in Table 1.

As shown in Figs. 15-17, the structure with all three types of dampers presents good performance under frequent earthquakes. While subjected to design and rare earthquakes, the viscous damper has a more superior performance in damage control than the others.

In Table 5, the acceleration limits of each device are given. Figure 18 shows the damage probability of operation room devices at the ground, third and eighth floor (the floor number has already been marked in Fig. 1). For operation room devices, the BRB and viscoelastic dampers have a similar control effect of structural acceleration and are better than the viscous damper. Figure 19 shows the damage probability of

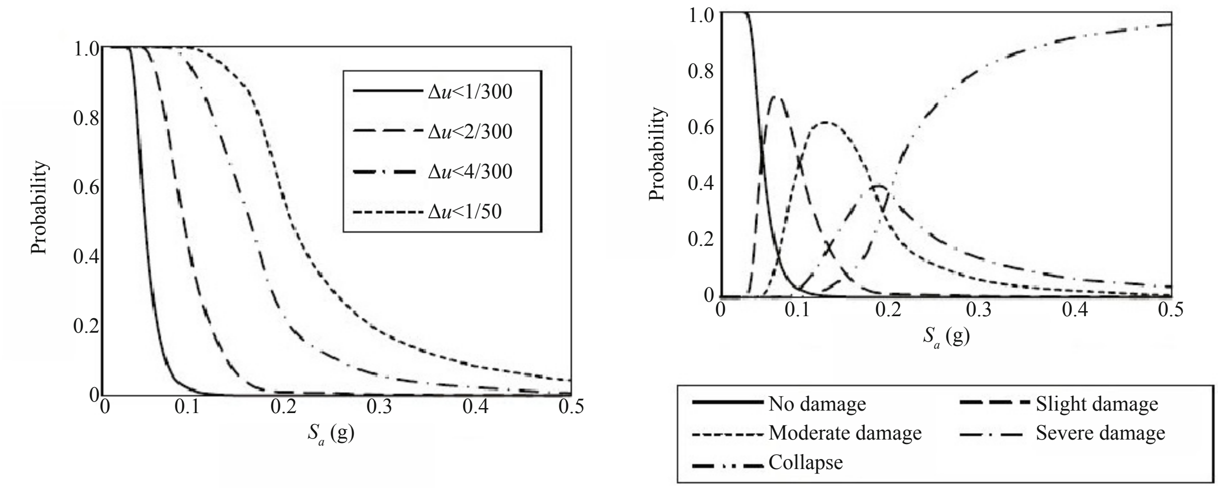

Fig. 12 (a) Fragility curves of structure with BRB dampers; (b) Performance curves of structure with BRB dampers

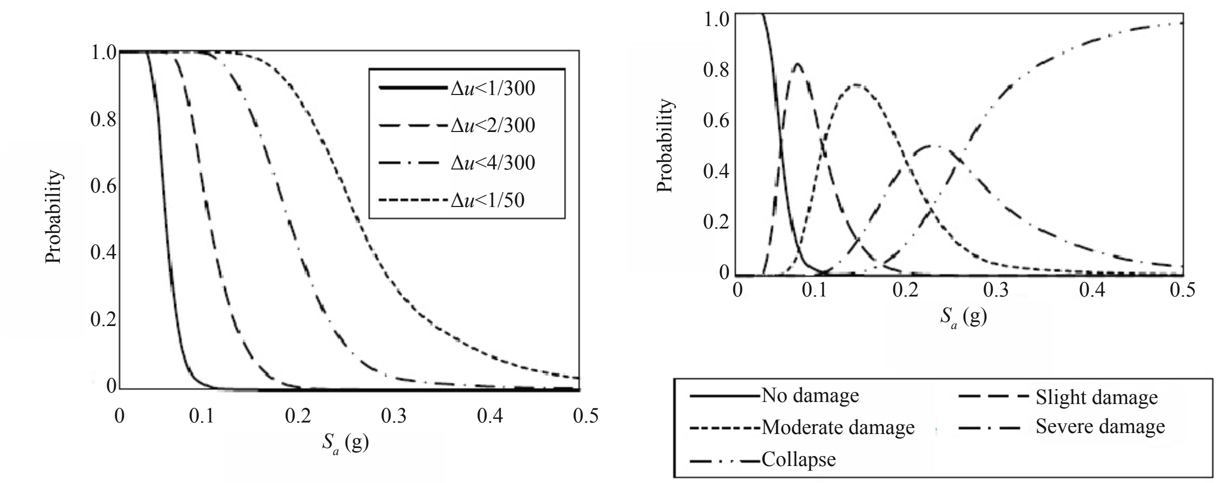

Fig. 13 (a) Fragility curves of structure with viscoelastic dampers; (b) Performance curves of structure with viscoelastic dampers

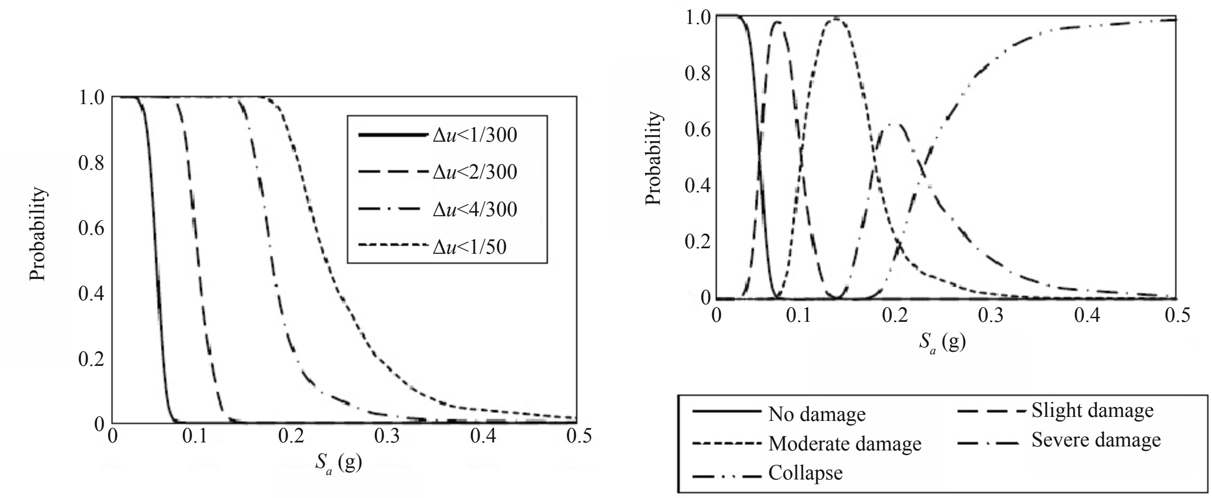

Fig.14 (a) Fragility curves of structure with viscous dampers; (b) Performance curves of structure with viscous dampers

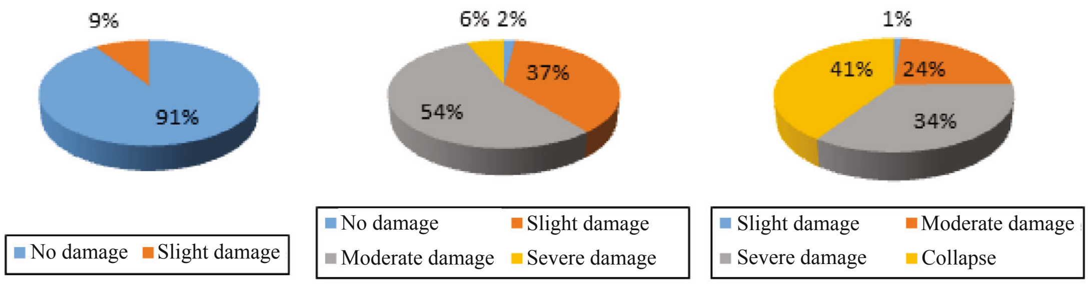

(a) Frequent earthquake (b) Design earthquake (c) Rare earthquake

Fig. 15 Damage probability of structure with BRB dampers under three levels of earthquakes

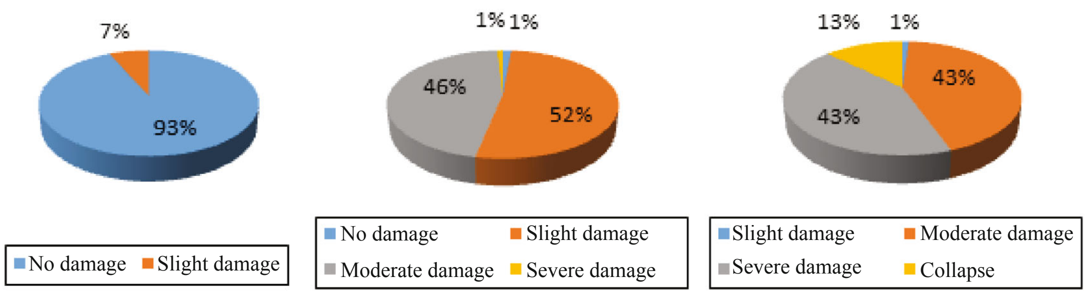

(a) Frequent earthquake (b) Design earthquake (c) Rare earthquake

Fig. 16 Damage probability of structure with viscoelastic dampers under three levels of earthquakes

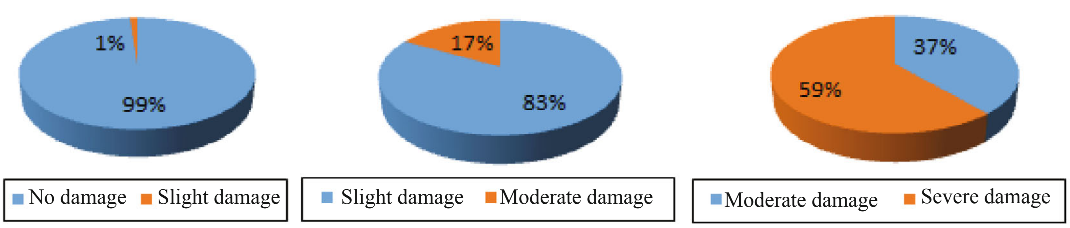

(a) Frequent earthquake (b) Design earthquake (c) Rare earthquake

Fig. 17 Damage probability of structure with viscous dampers under three levels of earthquakes

each type of device at the eighth floor. The BRB and viscoelastic damper also have similar performance in controlling acceleration, which are both better than the viscous damper. Figure 20 shows the damage probability of operation room devices at different floors and with different dampers. The result also shows that the damage probability decreases at higher floors.

Considering all the numerical analysis, the viscoelastic damper has the best control effect in collapse and acceleration. However, for damage control, viscous dampers are a better choice, and if it is necessary to consider acceleration control of devices, the BRB is also a good choice, but its damage control is not ideal.

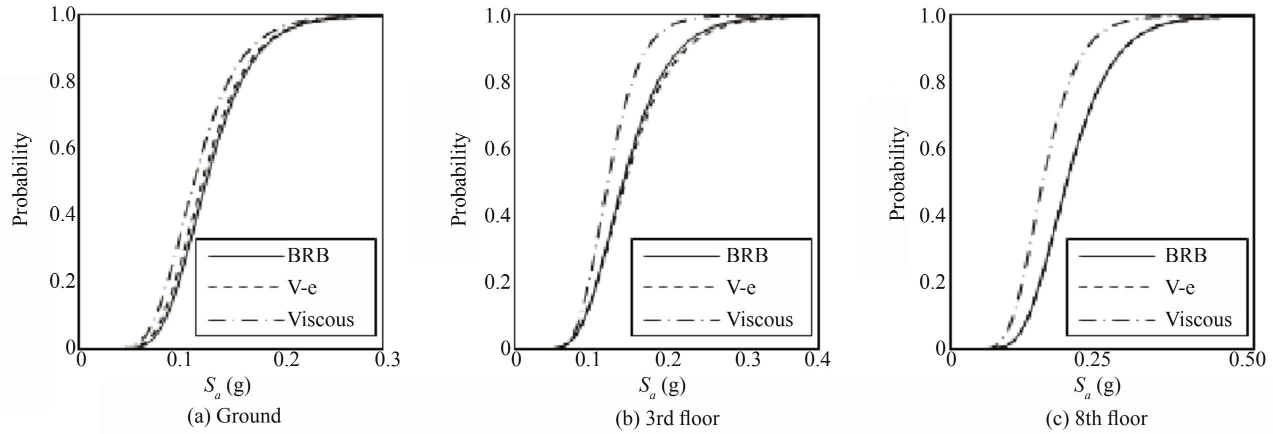

Fig. 18 Damage probability with dampers at ground, 3rd and 8th floor

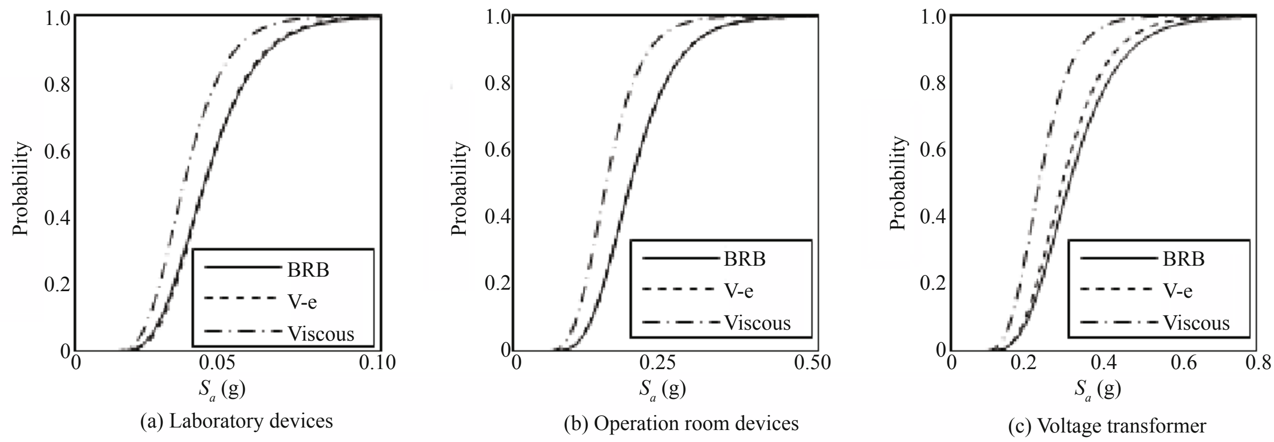

Fig. 19 Damage probabilities of different devices at 8th floor

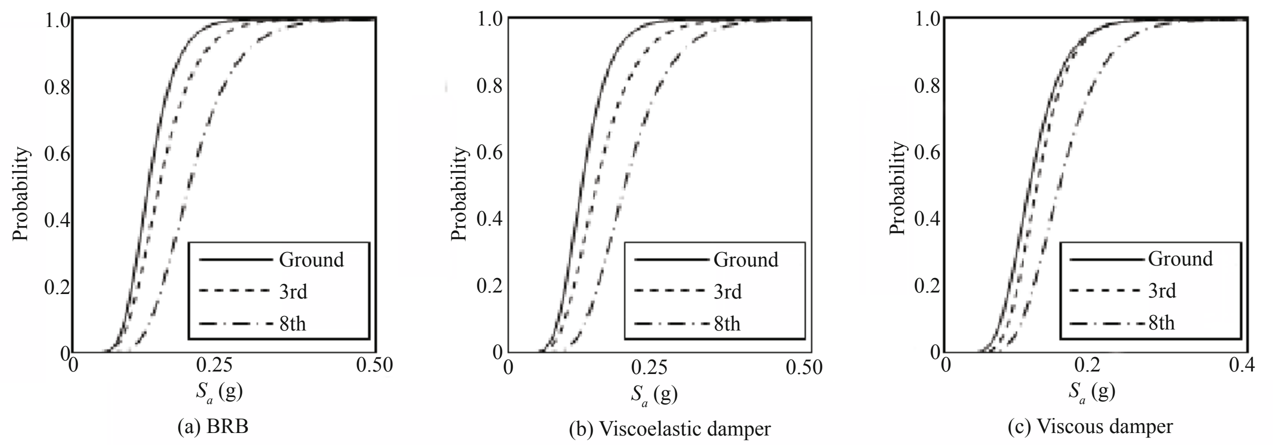

Fig. 20 Damage probabilities with the same damper at different floors (Operation devices)

3.3 Discussion on the design demands of the dampers

As is well known, structural failure in damped structures will probably happen quickly once the dampers are damaged and fail. In order to make the performance control useful and valuable as discussed in Section 3.2.2, it is necessary to design the ultimate displacement ratio to avoid failure. Due to the ultimate state level in Table 4, which is the value of 1/50 according to the Chinese code CSDB, the dampers in the first to ninth floor will experience 3,960 (story height) × 0.02 (drift ratio) × 0.91 (cos_theta) = 72.07 mm. Therefore, the ultimate displacement ratio of the dampers in this structure should be designed to be larger than $L/131$, in which the length of the damper is equal to 9,500 mm.

However, Fig. 21 shows hysteresis curves at several collapse-induced earthquake GRs for the three dampers according to the collapse analysis in FEMA P695, and each curve corresponds to the maximum relative displacement which is shown in Table 7. It shows that the ultimate displacement is about 90 mm according to the chosen GRs, and the displacement ratio equals $90/9500 = L/105$, which is larger than the value of $L/131$. Therefore, if the dampers are designed according to the performance control in CSDB, they would be damaged in the collapse analysis according to FEMA P695.

4 Conclusions

This study systematically evaluates the seismic performance of a structure with a supplemental viscoelastic damper, viscous damper and BRB. The different indexes are adopted in the evaluation, such as collapse state, displacement limits and acceleration limits. A steel structure benchmark model is adopted and all the dampers are designed based on the Chinese Building Design Codes (Guo *et al.*, 2011, Liu *et al.*, 2010). It is shown that even if dampers are designed according to the same displacement control target and same code, the seismic performance of the structure with different dampers may be obviously different from each other.

To achieve the optimal collapse control effect, the viscoelastic damper designed by Chinese codes is recommended, because it has the highest CMR values of all the dampers. Furthermore, its acceleration control effect is superior to the viscous damper, which is close to the buckling-restrained brace. Thus, the viscoelastic damper can be applied to control the collapse of the structure and protect important devices.

For damage control, the viscous damper has a better control effect than viscoelastic dampers. However, the collapse control acceleration control effect of the viscous damper is inferior to the other types of dampers. Therefore, it is a good choice to select viscous dampers designed by Chinese codes to reduce the displacement deformation of a structure.

collapse control effect is inferior to viscoelastic damper, and similar to viscous damper. Its displacement control is also inferior to viscoelastic damper and viscous

Table 7 Ultimate displacements of three dampers

Damper type	Ultimate displacement (mm)	Location	Ground record	Duration (s)
BRB	93.9501	2nd floor	Loma Prieta-1989	30
V-e damper	86.1668	2rd floor	Loma Prieta-1989	30
Viscous	96.2302	2th floor	Superstition Hills-02	30

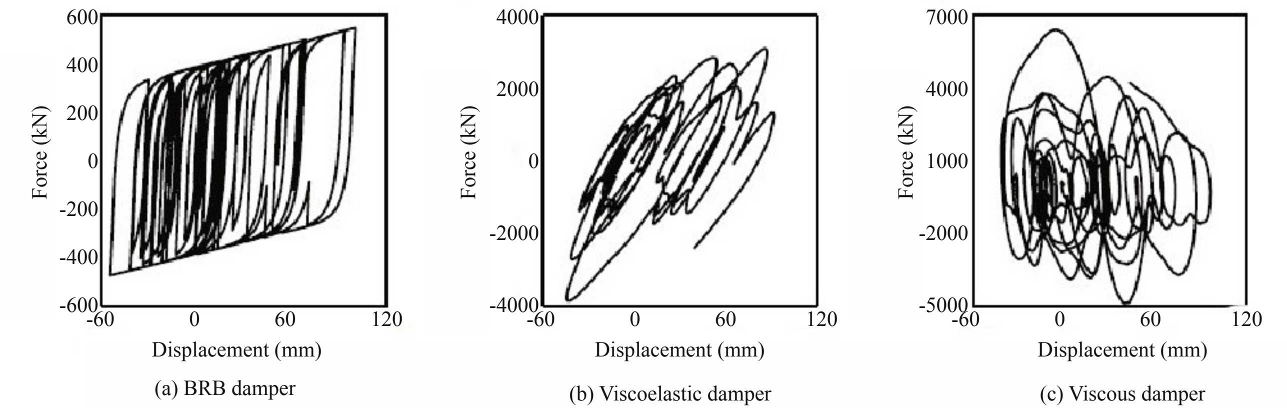

Fig. 21 Damper's hysteresis curve at the collapse-induced earthquake intensity

damper. However, its acceleration control effect is superior to viscous dampers and is closed to viscoelastic damper. So the buckling-restrained brace can be applied to acceleration control which is correlated to devices damage.

This paper evaluates viscoelastic damper, viscous damper and BRB designed by Chinese codes. Hence, the conclusions depend on not only dampers' own properties but also design codes and targets such as acceleration or displacement.

Acknowledgement

This work was supported by the National Natural Science Foundation of China (No. 51108466), Development Program for Changjiang scholars and innovative team (No. IRT1296) and the Project of Innovation-Driven Plan in Central South University. These supports are gratefully acknowledged.

References

ASCE-7-10, *Minimum Design Loads for Buildings and Other Structures*, American Society of Civil Engineering.

ASCE (2013), *Seismic Evaluation and Retrofit of Existing Buildings*, American Society of Civil Engineering.

Chang Kuo-Chun, Lin Yu-Yuan and Chen Chang-Yu (2008), "Shaking Table Study on Displacement-Based Design for Seismic Retrofit of Existing Buildings Using Nonlinear Viscous Dampers," *Journal of Structural Engineering*, **134**(4): 671–681.

Chiou Brian, Darragh Robert, Gregor Nick, *et al*. (2008), "NGA Project Strong-Motion Database," *Earthquake Spectra*, **24**(1): 23–44.

FEMA 451, *NEHRP Recommended Provision*, Federal Emergency Management Agency.

FEMA-P695 (2009), *Quantification of Building Seismic Performance Factors*, US Department of Homeland Security, FEMA.

Fu Yaomin and Kasai Kazuhiko (1998), "Comparative Study of Frames Using Viscoelastic and Viscous Dampers," *Journal of Structural Engineering*, **124**(5): 513–522.

GB50010-2010, *Code for Seismic Design of Buildings*, China Architecture & Building Press, Beijing. (in Chinese)

Gu Quan, Liu Yongdou, Guo Wei, *et al*. (2018), "A Practical Wheel-Rail Interaction Element for Modeling Vehicle-Track-Bridge Systems," *International Journal of Structural Stability and Dynamics*: 1950011.

Guo Wei, Li Hong-nan and Guo Zhen (2010), "Perturbation Spectrum Method for Seismic Analysis of Non-Classically Damped Systems," *Journal of Zhejiang University-SCIENCE A*, **11**(5): 325–334.

Guo Wei, Yu Zhi-Wu and Guo Zhen (2011), "Fast Stochastic Analysis for Non-Proportionally Damped System," *Mechanics Research Communications*, **38**(6): 468–470.

Guo Wei, Li Hong-nan, Liu Guo-huan, *et al*. (2012), "A Simplified Optimization Strategy for Nonlinear Tuned Mass Damper in Structural Vibration Control," *Asian Journal of Control*, **14**(4): 1059–1069.

Guo Wei, Yu Zhi-wu and Guo Zhen (2013), "An Efficient and Accurate Method for Calculating Stochastic Seismic Response of Non-Proportionally Damped Structure," *Journal of Structural Engineering*, **139**(3): 472–477.

Guo Wei, Yu Zhi-wu, Liu Guo-huan, *et al*. (2013), "Possible Existing Seismic Analysis Errors of Long Span Structures and Bridges while Utilizing Multi-Point Earthquake Calculation Models," *Bulletin of Earthquake Engineering*, **11**(5): 1683–1710.

Hou Wenqi, Li Yankun, Guo Wei, *et al*. (2018), "Railway Vehicle Induced Vibration Energy Harvesting and Saving of Rail Transit Segmental Prefabricated and Assembling Bridges," *Journal of Cleaner Production*, **182**: 946–959.

JGJ297-2013, "Technical Specification for Seismic Energy Dissipation of Building," *China Architecture & Building Press*, Beijing. (in Chinese)

Kasai K, Ito H, Motoyui S, *et al*. (2009), "Full-Scale Tests on Value-Added Performance of 5-Story Building with Various Dampers Commercially Available," *in 7th CUEE and 5th ICEE Joint Conference*, Tokyo Institute of Technology, 3–5 March 2010, Tokyo, Japan.

Kelly James M, Skinner RI and Heine AJ (1972), "Mechanisms of Energy Absorption in Special Devices for Use in Earthquake Resistant Structures," *Bulletin of NZ Society for Earthquake Engineering*, **5**(3): 63–88.

Li Gang and Li Hongnan (2004), "Experimental Study on Improved Mild Metallic Dampers," *Proceedings of the Third China-Japan-US Symposium on Structural Health Moni-toring and Control and Fourth Chinese National Conference on structural Control*.

Li Hong-Nan and Li Gang (2007), "Experimental Study of Structure with "Dual Function" Metallic Dampers," *Engineering Structures*, **29**(8): 1917–1928.

Liu GuoHuan, Guo Wei and Li HongNan (2010), "An Effective and Practical Method for Solving an Unnegligible Problem Inherent in the Current Calculation Model for Multi-Support Seismic Analysis of Structures," *Science China Technological Sciences*, **53**(7): 1774–1784.

Ohtori Y, Christenson RE, Spencer Jr BF, *et al*. (2004), "Benchmark Control Problems for Seismically Excited Nonlinear Buildings," *Journal of Engineering Mechanics*, **130**(4): 366–385.

SEAOC Vision-2000 (1995), *Performance-Based Seismic Design*, California RpbSEAo, Sacramento, CA.

Sun Feifei, Li Guoqiang, Guo Xiaokang, *et al*. (2011), "Development of New-Type Buckling-Restrained Braces and Their Application in Aseismic Steel Frameworks," *Advances in Structural Engineering*, **14**(4): 717–730.

Wang Xiaolin (2005), "Seismic Reliability Analysis for Functional Utility System in Hospital," *Master's Thesis*, Beijing University of Technology. (in Chinese)

Wu Bin, Zhang Jigang, Williams MS, *et al*. (2005), "Hysteretic Behavior of Improved Pall-Typed Frictional Dampers," *Engineering Structures*, **27**(8): 1258–1267.

Xiong Mingpan (2016), "Vulnerability Analysis Of High-Voltage Electrical Equipment Based on Ground Motion Parameter," *Master's Thesis*, Institute of Engineering Mechanics, China Earthquake Administration. (in Chinese)

Yu Zhiwu, Liu Hanyun, Guo Wei, *et al*. (2017), "A General Spectral Difference Method for Calculating the Minimum Safety Distance to Avoid the Pounding of Adjacent Structures During Earthquakes," *Engineering Structures*, **150**: 646–655.

Zhao Bin, Taucer Fabio and Rossetto Tiziana (2009), "Field Investigation on the Performance of Building Structures During the 12 May 2008 Wenchuan Earthquake in China," *Engineering Structures*, **31**(8): 1707–1723.

Zhao Junxian, Wu Bin and Ou Jinping (2011), "A Novel Type of Angle Steel Buckling-Restrained Brace: Cyclic Behavior and Failure Mechanism," *Earthquake Engineering & Structural Dynamics*, **40**(10): 1083–1102.

Zhao Zuozhou, Hu Yu and Qian Jiaru (2015), "Comparison of Ground Motion Selection Between Chinese and American Methods and Elasto-Plastic Time History Analysis of Frame-Core Wall Structures," *Journal of Building Structures*, **36**: 10–18.

Zhou Fulin, Cui Hongchao, ABE Shigetaka, *et al*. (2012), "Inspection Report of the Disaster of the East Japan Earthquake by Sino-Japanese Joint Mission," *Building Structure*, **4**: 002.

Zhou Yun, Deng Xuesong and Xu Zhaodong (2001), "Experimental Study on Properties of Lead-Viscoelastic Dampers," *Earthquake Engineering and Engineering Vibration*, **1**: 025.